NWP SAF
Microwave transmittance models for RTTOV

P.J. Rayer
SA Section, NWP Division, Met Office

This documentation was developed within the context of the EUMETSAT Satellite Application Facility on Numerical Weather Prediction (NWP SAF), under the Cooperation Agreement dated 25 November 1998, between EUMETSAT and the Met Office, UK, by one or more partners within the NWP SAF. The partners in the NWP SAF are the Met Office, ECMWF, KNMI and Météo France.

Forming part of NWP SAF Deliverable 8.1			
Change record			
Version	Date	Author / changed by	Remarks
1	12 Feb 2001	P.J. Rayer	

1. INTRODUCTION

This report is concerned with the calculation of spectral transmittances through the atmosphere in the microwave region using a radiative transfer model (RTM) that adopts a line-by-line (LbL) approach. The context for the NWP SAF is that, when averaged over the microwave channels of a satellite radiometer, such transmittances are needed to determine coefficients for the fast RTM that will be used in assimilation schemes for numerical weather prediction (NWP).

RTTOV (*Eyre*, 1991, *Saunders* et al. 1999a, 1999b) is a 'broadband' fast RTM in the sense that, when it sets up the radiative transfer equation (RTE), the spectral quantities that would ordinarily appear are all replaced by appropriate channel averages. In this way, the model will simulate a measurement made by the instrument without the need for any on-line channel averaging. The integration of the RTE along the viewing path takes place in the 'radiance stage' of the model, and requires the set of channel transmittances from each level to space. These are averages of the underlying transmittance spectrum with the channel response functions of the instrument, and are calculated in the preceding 'transmittance stage' of the model.

RTTOV is fast because the transmittance stage is parametrized. This involves a set of predictor functions of the atmospheric state variables that are weighted by coefficients that depend on the channel characteristics. To determine these coefficients for each new satellite instrument, regression data come, in the current version, from a known set of 43 diverse profiles (the dependent set) for which channel transmittances are already available.

To obtain these channel transmittances, an existing archive of transmittance spectra calculated off-line for the dependent profiles using an LbL RTM will have been customized for each new instrument by averaging over its channel response functions. One aim of this report is to examine whether certain product-rules remain valid when using a channel transmittance The other aim is to compare two different microwave LbL models for calculating the absorption coefficient that will determine the spectral transmittance for the dependent set.

2. MICROWAVE TRANSMITTANCE MODELS

The series of millimetre-wave propagation LbL RTMs developed by Liebe and several different collaborators during the last two decades (e.g. *Liebe* et al. 1989, 1992, 1993), here abbreviated to MPM with year appended, are often used as the basis for LbL atmospheric calculations at microwave frequencies. For instance, the LbL model presently used by the Met Office in determining the coefficients for RTTOV-6, the current version of the fast model described on the NWP SAF website `http://www.metoffice.com/sec5/NWP/NWPSAF/rtm/`, is a hybrid MPM model on 43 pressure levels that we shall refer to here as simply MPM. To calculate the spectral absorption coefficient on each level, this model (see Appendix 1) calls a water vapour subroutine based upon MPM-1989 and a dry-air subroutine based upon MPM-1993, but adjusted so that the dry-air calculation effectively comes from MPM-1992.

Another LbL RTM for the microwave (*Rosenkranz* 1998) has been developed recently at Massachusetts Institute of Technology (MIT) by Dr P.W. Rosenkranz, who has supplied the code for this study. Although the model is complete in the sense that there is code to deal with surface effects, the geomagnetic field, and radiative transfer, only the calculation of the spectral absorption coefficient in each atmospheric layer is used here. For this, the MIT model

is provided with a water vapour function subprogram and two dry-air function subprograms for oxygen and nitrogen.

The spectral line parameters used in MPM and MIT are discussed (with conversion factors) in Appendices 2 and 3, and the continua for dry-air and water vapour are discussed in Appendix 4. To summarize here, the models use (almost) the same line parameters (H_2O from MPM-1989, O_2 from MPM-1992), but in different units and with not entirely coincident line selections. Both models use the same expression for the O_2 absorption coefficient (but factored somewhat differently), and the same is true for H_2O, except that MIT truncates the line shape, a legacy from the need to perform comparisons that include the CKD-continuum (*Clough et al.* 1989). However, whereas MPM uses the continuum formulated in MPM-1989, the MIT model, as supplied, uses the MPM-1989 foreign continuum (adjusted to compensate for line truncation) and a self continuum based on a low-frequency approximation (valid below 800 GHz) of MPM-1993.

For comparison purposes, a version of MPM was coded with a switch (see Appendix 1) for calling either the two MPM absorption subroutines (water vapour and dry-air), or two new subroutines that perform several unit conversions before calling the three corresponding MIT function subprograms (water vapour, oxygen, nitrogen) as supplied. Simulations of channel transmittances for the AMSU, SSM/I and TMI instruments were then performed on the 43 profiles of the RTTOV-6 dependent set.

3. APPROXIMATIONS IN TRANSMITTANCE MODELS

In a strict simulation of observations by a given radiometer, the spectral radiance delivered to the instrument as calculated by the LbL model should be averaged over the channel response function. In a fast model like RTTOV-6, it is more usual to choose a representative Planck function for each channel, since this is a smooth function, and include all the channel averaging within the transmittance from each level to space.

However, the regression that provides the RTTOV-6 coefficients does not use these channel transmittances directly. Rather, as can be seen from (1), their ratio for adjacent levels provides an *effective* transmittance τ_L across the intervening layer, and the negative logarithm of this is the corresponding *effective* layer optical depth d_L. This is the most basic quantity predicted in the RTTOV transmittance stage, and we have

$$\tau_L \stackrel{\text{def}}{=} \frac{\tau_{j-1}}{\tau_j}, \qquad d_L \stackrel{\text{def}}{=} -\log \tau_L, \qquad \hat{d}_L = \sum_i c_i P_i, \qquad \hat{\tau}_j = \exp[-\sum_{\text{path}} \hat{d}_L], \tag{1}$$

in which the first two relations are local definitions, and the last two relations (with carets appended) are predictive. The quantity d_L is only an 'effective' layer optical depth in the sense that its construction, based on a ratio taken *after* channel averaging, prevents its prediction from local quantities alone, since the overlying path to space is also involved to some extent. By the same token, once all the layer predictions have been made, exponentiation followed by an *exact* product-rule, written as a sum of exponents in the path summation in (1), will provide the corresponding channel averaged transmittance to space required for the RTE.

The exactness of the product rule in the last relation shown in (1) is really a consequence of internal consistency. There will, nevertheless, have been various approximations involved in the LbL calculations from which τ_L was derived, including various representativeness errors relating to the spectral grid of frequencies across the channel width, the vertical grid of levels in the atmospheric profile, the layer values adopted for the profile variables, and the atmospheric profile set itself. These matters are not addressed in this report. Rather, attention remains focused in this section on two further problems for MPM regarding the channel averaging.

The first problem concerns the fact that the original release of RTTOV-6, since superseded, used what will here be called old-MPM in the generation of its coefficients. In old-MPM, and several related LbL codes presently in use for the microwave, calculated layer optical depths for the input profile are averaged *directly* over the channel response functions. This is *before* path cumulation from each level to space and subsequent exponentiation for the corresponding transmittances. The effect is to remove the channel averaging one step further from the radiance (i.e. from transmittance to attenuation) and, although it may lead to simpler coding, it also involves an approximation that is unwarranted unless the differences turn out to be very small.

The second problem arising from the channel averaging concerns the product rule whereby transmittances relating to separate absorbing gases, here uniformly mixed gases (together) and water vapour, are multiplied together for the total, a procedure that should be applied only to spectral quantities, before channel averaging. Possible problems with this are circumvented in MPM by defining suitable quantities to replace the channel transmittances so that they do indeed satisfy this product-rule. For mixed gases, which here means dry-air, MPM defines the channel transmittance in the usual way. For water vapour, however, a *ratio* is formed of the total transmittance to the mixed gas transmittance (*Susskind et al.* 1983). By definition, the product-rule for gases will now be *exact*, despite the channel averaging.

It is, however, pointless to move to predicting a ratio for water vapour in this way without at the same time moving to transmittance before performing the channel average. After all, if one is doing no more than adding exponents, the answer will be the same whether performed before or after averaging the exponents. In old-MPM, therefore, the use of a ratio has no effect at all.

This can be summarized as follows. Suppose we use 'MG' and 'WV' to denote the attenuation from some level to space due to mixed gases and water vapour respectively, with τ_{MG} and τ_{WV} for the corresponding transmittance in each case, and suppose we then use angle-brackets to indicate spectral averaging over the channel response function. If, in addition, we use τ_{DIR} and τ_{WR} to indicate, respectively, the transmittance for *all* gases taken together in a direct calculation and that for the water vapour alone *when defined by the ratio mentioned above*, then old-MPM will have

$$\tau_{MG} \stackrel{\text{def}}{=} e^{-\langle MG \rangle}, \qquad \tau_{WV} \stackrel{\text{def}}{=} e^{-\langle WV \rangle}, \qquad \tau_{DIR} \stackrel{\text{def}}{=} e^{-\langle MG+WV \rangle},$$

$$\tau_{WR} \stackrel{\text{def}}{=} \frac{\tau_{DIR}}{\tau_{MG}} = \frac{e^{-\langle MG+WV \rangle}}{e^{-\langle MG \rangle}} = e^{-\langle MG+WV \rangle - \langle MG \rangle} = e^{-\langle WV \rangle} = \tau_{WV}, \tag{2}$$

which confirms that the use of a ratio with these definitions has no effect. This is also confirmed in Table 1, which shows old-MPM values for part of the reference transmittance profile.

TABLE 1.
Transmittance to space from the lowest three levels of the reference profile (No.43) for AMSU channel 20 . Spectral averaging has been performed over optical depth (old-MPM case), so there is no difference between the last two columns.

All Gases	Mixed Gases	Water Vapour	Water Vapour Ratio
.196338	.979223	.200503	.200503
.174964	.978518	.178805	.178805
.167075	.978233	.170793	.170793

By contrast, from MPM itself, in which the channel averaging has been moved more properly to the transmittance, we have

$$\tau_{MG} \overset{\text{def}}{=} \left\langle e^{-MG} \right\rangle, \qquad \tau_{WV} \overset{\text{def}}{=} \left\langle e^{-WV} \right\rangle, \qquad \tau_{DIR} \overset{\text{def}}{=} \left\langle e^{-(MG+WV)} \right\rangle,$$

$$\tau_{WR} \overset{\text{def}}{=} \frac{\tau_{DIR}}{\tau_{MG}} = \frac{\left\langle e^{-(MG+WV)} \right\rangle}{\left\langle e^{-MG} \right\rangle} \neq \tau_{WV}, \tag{3}$$

so here there is indeed an effect in using the ratio. MPM values illustrating (3) and corresponding to those in (2) are shown in the last two columns of Table 2.

TABLE 2.
As for Table 1, but with the spectral averaging performed over transmittance (MPM case). The main difference from Table 1 (old-MPM) is the change in column one, but notice also the small difference now arising between the last two columns.

All Gases	Mixed Gases	Water Vapour	Water Vapour Ratio
.202070	.979223	.206334	.206357
.180787	.978519	.184732	.184756
.172920	.978233	.176745	.176768

The schemes shown in (2) and (3) both work with internally consistent definitions, both satisfy the product rule $\tau_{DIR} = \tau_{MG} \times \tau_{WR}$, and actually both show very little difference when τ_{WV} is used in place of τ_{WR}. However, only in (3) does the resulting value for τ_{DIR} represent the channel averaged transmittance properly defined, and the resulting difference in equivalent black body brightness temperature (TB) between the two schemes is shown, averaged over all profiles, in Table 3.

TABLE 3.

Comparison (MPM – Old-MPM) based on the brightness temperature in kelvin for the AMSU channels as calculated for the RTTOV dependent profile set using appropriate channel emissivities. In old-MPM the channel averaging is performed on optical depth, while in MPM it is done on transmittance. Columns 2-4 give the average difference (bias), the root-mean-square difference, and the standard deviation (excludes bias). Columns 5-6 give the maximum difference and the profile involved. Columns 7-8 give the brightness temperature as calculated for the reference profile.

AMSU	Δ TB	rms TB	sd TB	max Δ TB	max prof	MPM	Old-MPM
1	.00	.00	.00	.00	6	129.22	129.22
2	.00	.00	.00	.00	10	134.97	134.97
3	.00	.00	.00	.00	28	207.09	207.09
4	–.08	.08	.01	–.11	3	240.50	240.59
5	–.01	.03	.02	–.05	36	241.58	241.59
6	.19	.20	.07	.32	3	231.38	231.18
7	.24	.27	.12	.42	2	223.52	223.29
8	.16	.20	.11	.34	13	218.22	218.10
9	.03	.08	.07	.16	12	215.15	215.14
10	–.07	.21	.20	–.53	23	217.40	217.48
11	–.33	.47	.33	–.92	32	222.79	223.07
12	–.54	.68	.42	–1.50	34	231.13	231.59
13	–.80	1.01	.63	–2.16	36	241.14	241.90
14	–.46	.72	.56	–1.50	33	247.43	247.93
15	.00	.00	.00	–.01	6	186.66	186.66
16	.00	.00	.00	–.01	6	186.65	186.65
17	.00	.00	.00	–.01	1	216.94	216.95
18	.05	.07	.06	.15	6	239.99	239.93
19	.02	.12	.12	–.20	37	251.78	251.69
20	–.04	.11	.11	–.22	39	258.87	259.00

4. RESULTS FOR MPM ON CHANGING AVERAGING PROCEDURE

This comparison concerns the brightness temperature (TB) differences observed in moving the channel averaging from the attenuation (in old-MPM) to the transmittance (in MPM). The transmittance output obtained directly from old-MPM and MPM was used, and a separate postprocessing routine was written to convert this to the corresponding TBs for a specified set of surface variables. TB statistics are shown for each channel in Table 3, but averaged over the profile set in the form of the TB difference (MPM − old-MPM), its root-mean-square (rms) and its standard deviation. The channel TBs for the reference profile are shown alongside for convenience, and a bar-chart of the data is shown in Fig.1.

At the level of accuracy shown in Table 3, there is no change in the windows (channels 1-3 and 15-17) because there is no significant spectral variation across the channel. However, as characteristic weighting functions climb channel-by-channel (4-14) through the more structured oxygen band, differences become larger. The mid-tropospheric temperature sounding channels 6-8 show a small average warming in TB of 0.2 K in the move from old-MPM to MPM (standard deviation around 0.1 K). However, the very narrow stratospheric channels 11-14 have narrow sidebands located on the steep climb towards the peaks of a pair of adjacent lines of the band. Here there is a cooling effect, the largest average reduction in TB being 0.8 K in channel 13 (standard deviation around 0.6 K), with a maximum of several kelvin.

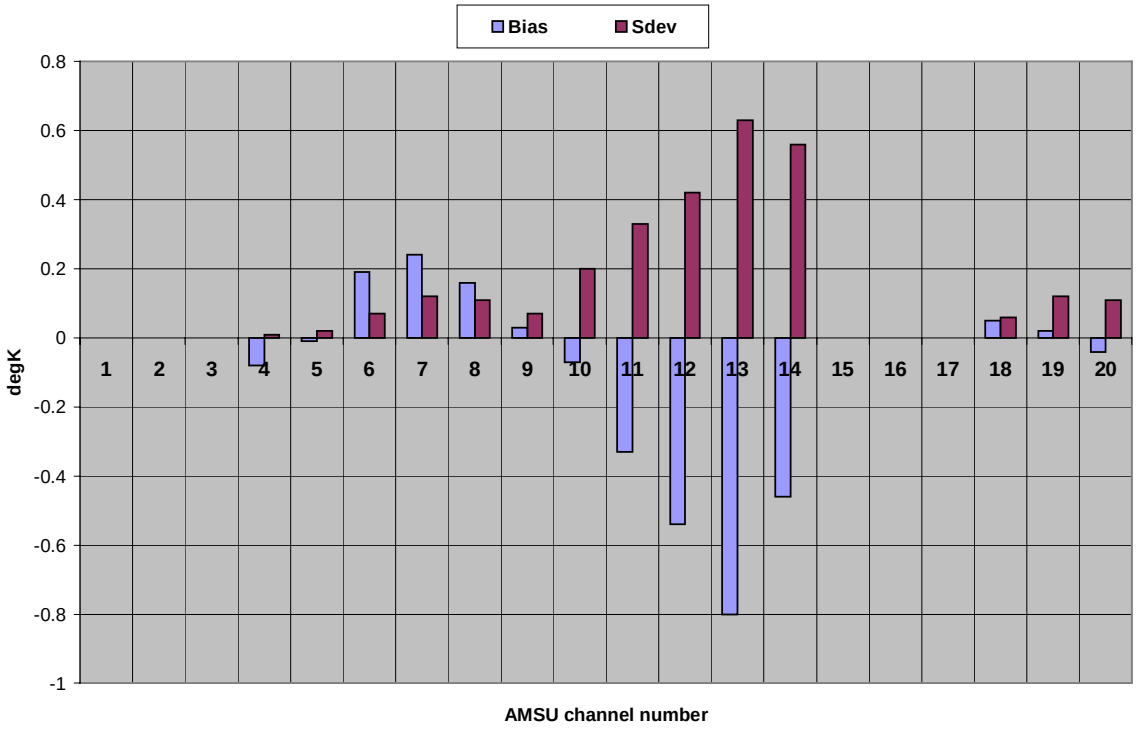

FiGURE 1 *Brightness temperature difference statistics in kelvin for (MPM − old-MPM), where old-MPM performs the spectral averaging on optical depth, while MPM does it on transmittance.*

In Figs.2-3 below, the vertical coordinate is the level number counted from top of atmosphere, and the corresponding pressures are given in Table 4.

TABLE 4
Pressure levels for the dependent set of profiles numbered from the top. The level numbers provide the vertical coordinate in Figs.2-3 and 5—7.

Level	Pressure hPa	Level	Pressure hPa	Level	Pressure hPa
1	0.100	15	69.970	29	478.540
2	0.290	16	85.180	30	521.460
3	0.690	17	102.050	31	565.540
4	1.420	18	122.040	32	610.600
5	2.611	19	143.840	33	656.430
6	4.407	20	167.950	34	702.730
7	6.950	21	194.360	35	749.120
8	10.370	22	222.940	36	795.090
9	14.810	23	253.710	37	839.950
10	20.400	24	286.600	38	882.800
11	27.260	25	321.500	39	922.460
12	35.510	26	358.280	40	957.440
13	45.290	27	396.810	41	985.880
14	56.730	28	436.950	42	1005.430
				43	1013.250

Figs.2-3 show how the profile of transmittance to space changes in the AMSU channels most affected, this being averaged over the profile set for the statistic (MPM − old-MPM) × 100. The comparison therefore measures the difference in transmittance expressed as a percentage of unit transmittance. The rms difference is almost all bias and amounts to a small transmittance increase of between 0.02 and 0.03 in each case. The peak in the difference appears to rise from channel to channel with that of the weighting function, although the greatest dispersion, still very small indeed, occurs a little above this level each time.

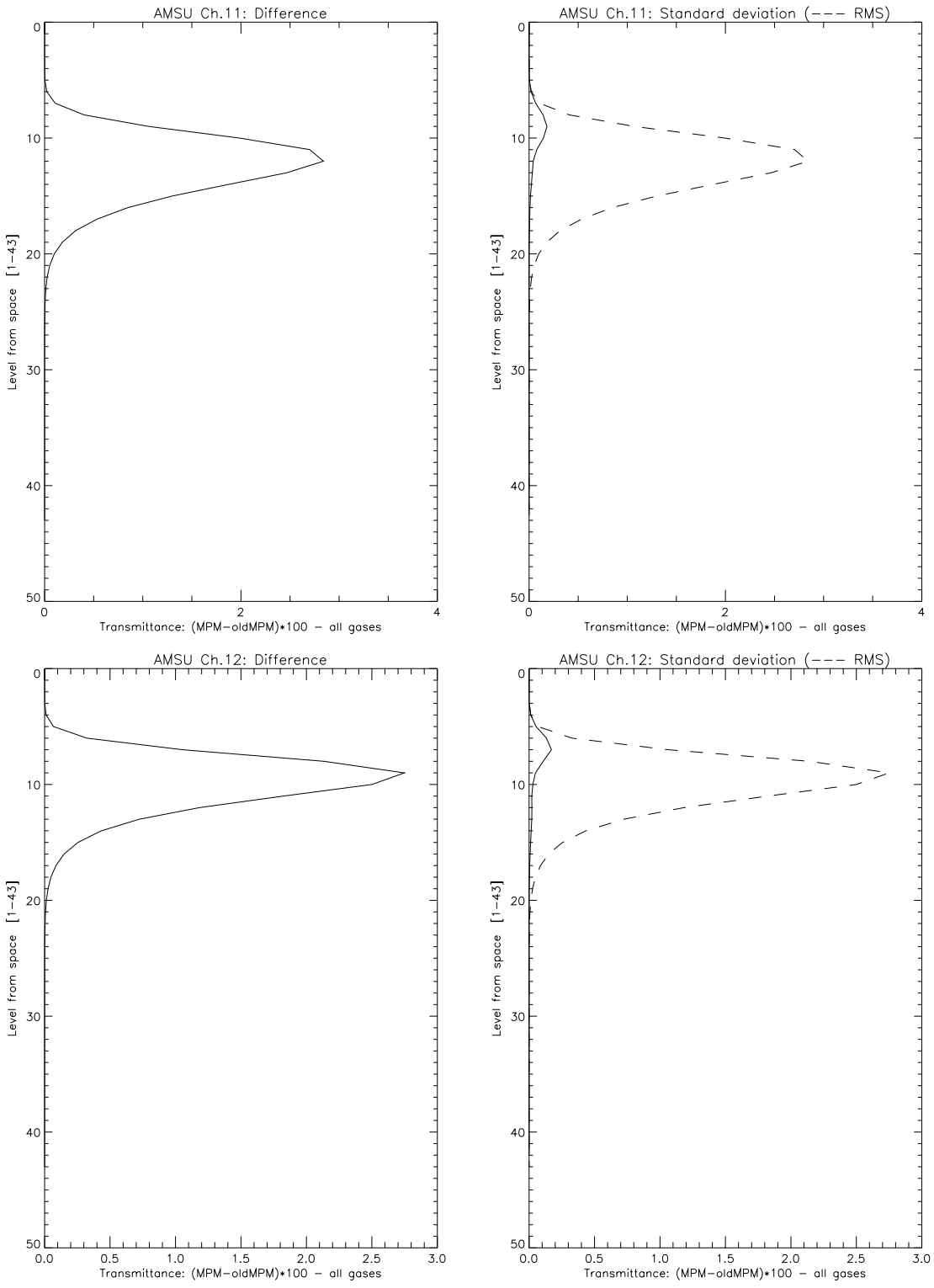

FIGURE 2. *For AMSU channels 11-12, mean and dispersion of the transmittance differences (×100) between MPM, which performs the spectral averaging on transmittance, and old-MPM, which uses optical depth. The ordinate is the profile level number from 1 (top) to 43 (bottom) as shown in Table 4. Dispersion, shown as standard deviation, is the solid contour on the right.*

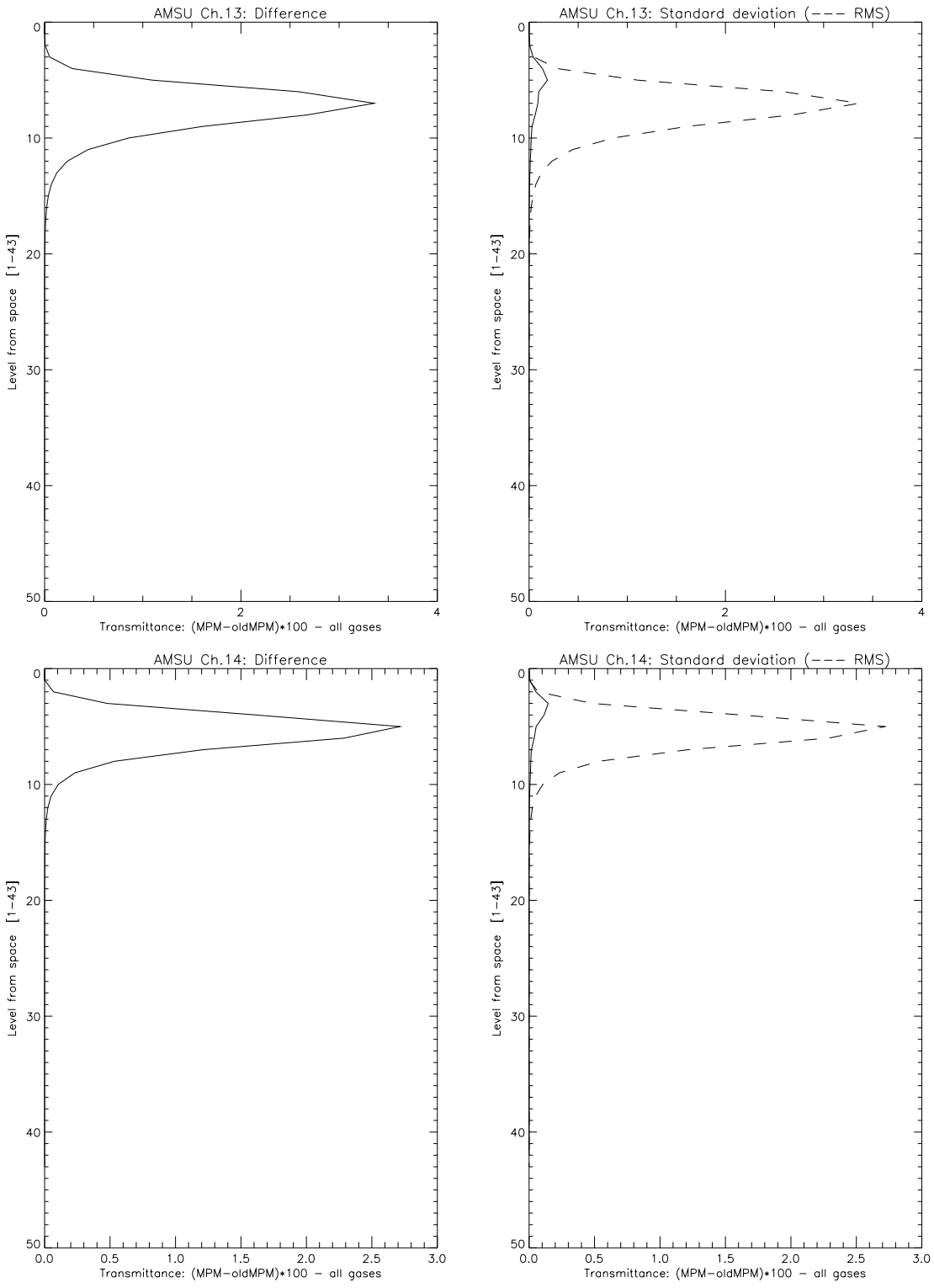

FIGURE 3. *As Figure 2, but for AMSU channels 13-14.*

5. COMPARISON OF MPM WITH MIT MODEL

The comparison of the predictions of the MIT and MPM models is now considered. The first calculations showed large differences in the high-peaking temperature sounding channels, as shown in Table 5. After making the changes described below, the much closer agreement shown in Table 6 was obtained.

TABLE 5

Layout as for Table 3, but for (MIT – MPM), both models here performing the spectral averaging on transmittance. TheAMSU channels shown are those with largest anomalous differences.

AMSU	ΔTB	rms TB	sd TB	max ΔTB	max prof	MIT	MPM
10	–0.04	0.05	0.03	–0.09	41	217.36	217.40
11	–0.14	0.18	0.11	–0.33	36	222.66	222.79
12	–0.35	0.52	0.38	–1.04	28	230.79	231.13
13	–0.31	1.16	1.12	–2.88	33	240.79	241.14
14	1.48	2.71	2.27	6.66	34	248.87	247.43

TABLE 6.

Layout as for Table 3, but for (MIT – MPM) correcting Table 5. The scalar Zeeman approximation to allow for the geomagnetic filed has been removed from MPM for consistency with MIT, and the O_2 set of line parameters in MPM has been slightly amended to agree with the published version.

AMSU	ΔTB	rms TB	Sd TB	max ΔTB	max prof	MIT	MPM
1	–.11	.16	.11	–.37	5	129.07	129.24
2	.07	.23	.22	.91	8	134.90	135.00
3	.07	.24	.23	.94	8	207.05	207.15
4	.02	.06	.06	.23	8	240.50	240.52
5	.01	.02	.01	.05	8	241.56	241.56
6	.00	.00	.00	.01	6	231.37	231.37
7	.00	.00	.00	.00	23	223.52	223.52
8	.00	.00	.00	.00	9	218.22	218.22
9	.00	.01	.01	.01	23	215.14	215.14
10	.01	.01	.01	.02	32	217.48	217.48
11	.01	.01	.01	.03	34	222.66	222.65
12	.02	.02	.01	.03	36	230.79	230.78
13	.01	.02	.01	.04	36	240.79	240.77
14	.01	.01	.01	.03	33	248.87	248.85
15	.17	.72	.70	2.27	8	186.04	186.53
16	.17	.73	.70	2.28	8	186.03	186.53
17	.01	.50	.50	1.66	2	216.16	216.96
18	.05	.13	.12	–.29	40	240.11	239.99
19	–.03	.20	.20	–.40	40	251.90	251.78
20	–.14	.28	.25	–.46	37	258.82	258.87

The large differences in Table 5 were unexpected. MIT uses O_2 line parameters from MPM-1992 (almost) as published and MPM was, for Table 5, using a very closely related set. As detailed in Appendix 2, the literature indicates that MPM-1993 uses a slight rescaling of the

MPM-1992 widths and line coupling coefficients for O_2 (Appendix 2). For Table 5, this rescaling had been reversed in MPM, but this left some small differences from the line parameters published for MPM-1992. Although, for all subsequent work, MPM was installed with the MPM-1992 parameters as published, most of the difference with MIT shown in Table 5 still remained and required explanation.

It was thought that MPM made no allowance for the geomagnetic field, so the set of Zeeman routines supplied with MIT had been omitted from the comparison. In the Zeeman effect, the geomagnetic field splits each O_2 line into a multiplet, and this will alter the transmittance in channels that see contributions from high enough in the stratosphere, where pressure broadening is very much reduced. An examination of the MPM code provoked by Table 5 revealed the presence (in a single statement) of a scalar approximation to the Zeeman effect representing the (unnumbered) equation provided in *Liebe et al.* (1993) for that purpose (Sec.2.2.1, p.2). When the statement was removed from MPM, the results for the two models were much more compatible, as shown in Table 6. . In fact, the scalar approximation in MPM used the upper-bound polar value of 60 μT (0.6 gauss) for the geomagnetic field for every profile, whereas 22-65 μT would be the appropriate range over location and altitude.

In Table 6 the TB difference statistics are shown by channel, together with the corresponding TB from the reference profile, and a bar-chart of the data can be seen in Fig.4.

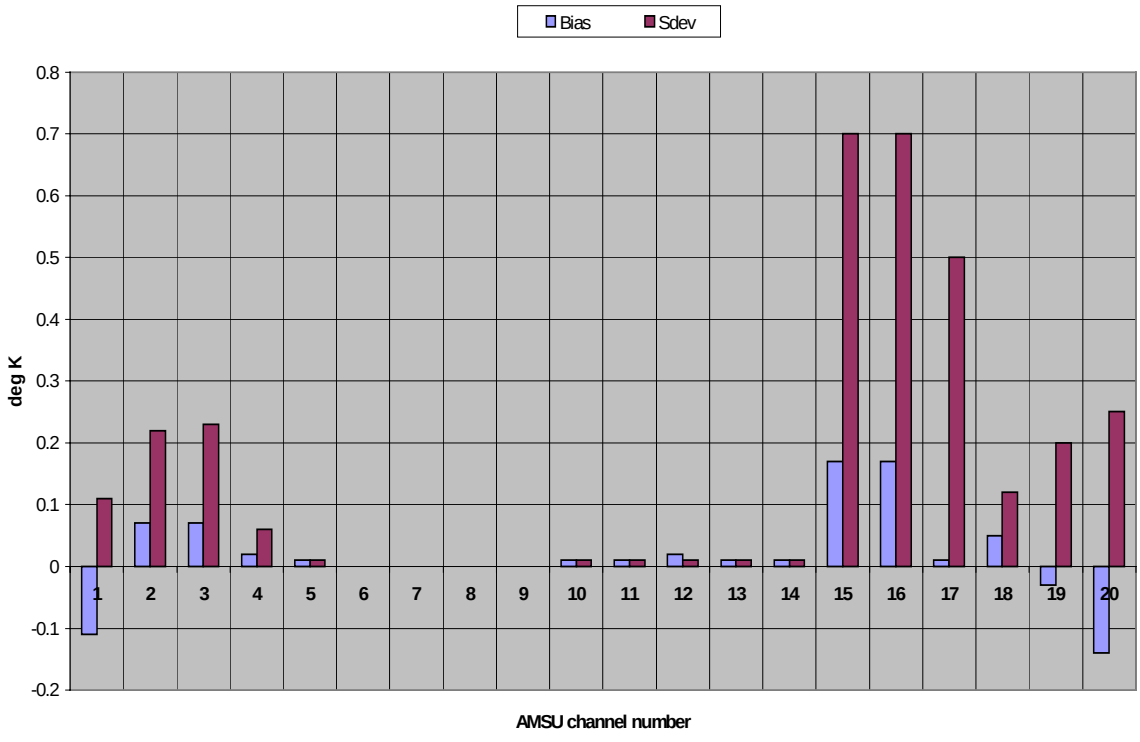

FIGURE 4 *Brightness temperature difference statistics in kelvin for (MIT – MPM), where both the MIT and MPM models perform the spectral averaging in transmittance.*

Since the oxygen line parameters used are very similar (see Appendix 2), differences are very small in the main temperature sounding channels. The water vapour line parameters are also very similar (see Appendix 3), and the larger differences seen in window channels 1-5, 15-17 are due to the continuum contribution, and to the self continuum in particular (see Appendix 4). In fact, although the standard deviation is about 0.7 K in channels 15-16, the maximum difference across the profile set amounts to several kelvin.

Figs.5-7 show how the profile of transmittance to space changes in the AMSU channels most affected, this being averaged over the profile set for the statistic (MIT − MPM) × 100. As in Figs.2-3, therefore, the comparison measured the difference in transmittance expressed as a percentage of unit transmittance with the vertical coordinate being the level number counted from top as given in Table 4.

Fig.5 shows the effect on the low frequency window channels 2 and 3 (31 and 50 GHz). In moving from MPM to MIT, the atmospheric column has become very slightly more transparent between about 650 and 750 hPa and very slightly less transparent everywhere else. The effect is very small, and probably reflects the redistribution of contributions within the weighting function due to the change in the temperature dependency of the self-continuum --- see Appendix 4 Eqs 4-5. In Fig.6, which shows the higher frequency window channels 16-17 (89 and 150 GHz), the situation is qualitatively very similar but greater in amplitude.

Fig.7 shows the two most affected channels (19-20) on the 183 GHz water vapour line. These, have sidebands less centrally located than channel 18, and therefore more sensitive, for a given pressure and humidity, to the temperature dependency of the line halfwidth. However, since the line parameters were very similar for the two models, this is not the cause. Rather, it is much more likely that the change in the self-continuum is again revealed here. Although these channels show much less dispersion at lower levels than in Fig.6, the amplitude of the difference is somewhat larger. Despite being larger in absolute terms, these changes form a much smaller part of the overlying transmittance than in the windows, and therefore have a smaller effect on the upwelling radiation transferred to the top of the atmosphere, as can be seen in Fig.4.

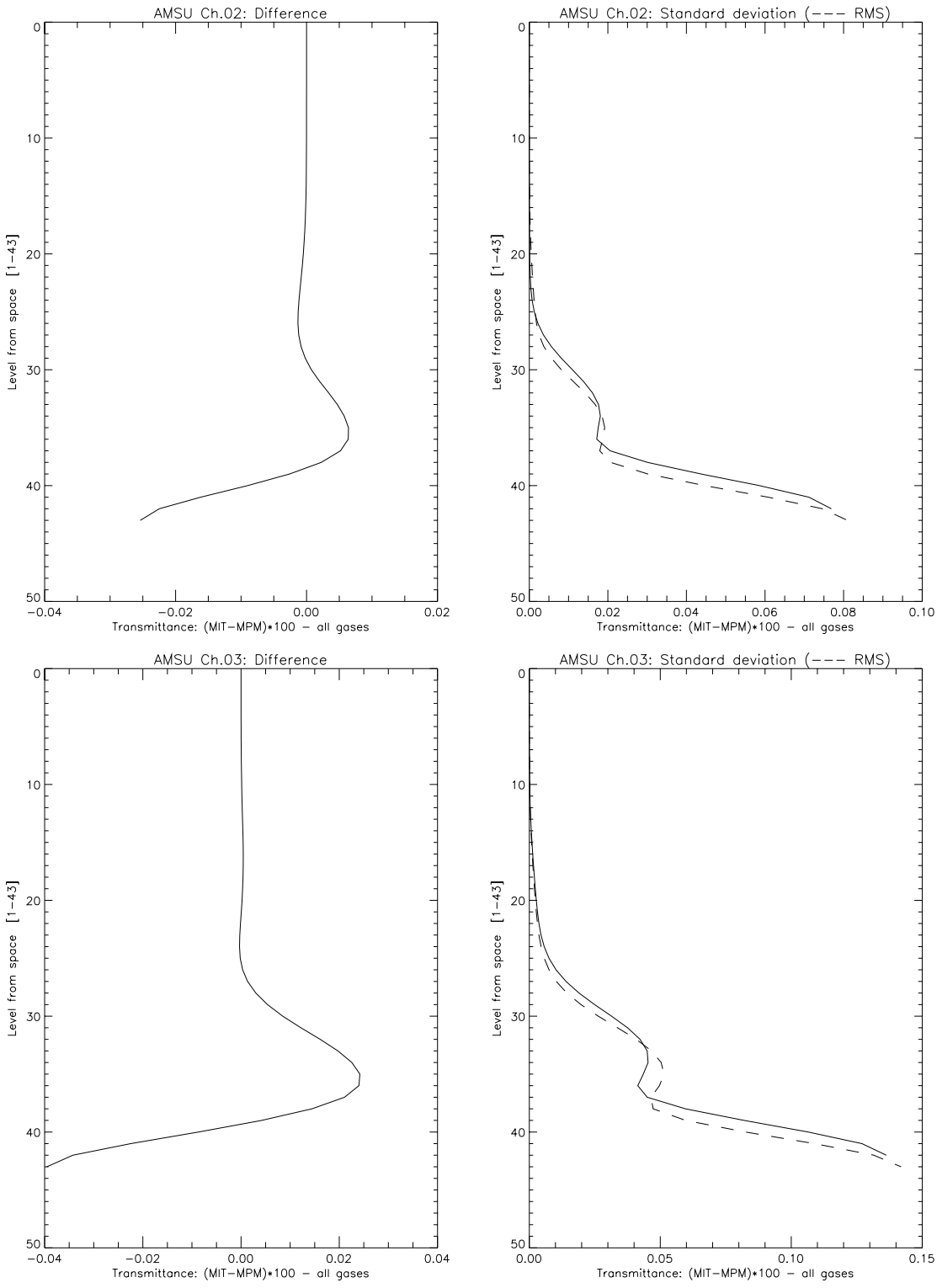

FIGURE 5. *For AMSU channels 2-3, mean and dispersion of the transmittance differences (×100) between the MIT model and MPM, both performing the spectral averaging on transmittance. As in Figures 2-3, the ordinate is the profile level number from 1 (top) to 43 (bottom) as shown in Table 4 and dispersion, shown as standard deviation, is the solid contour on the right.*

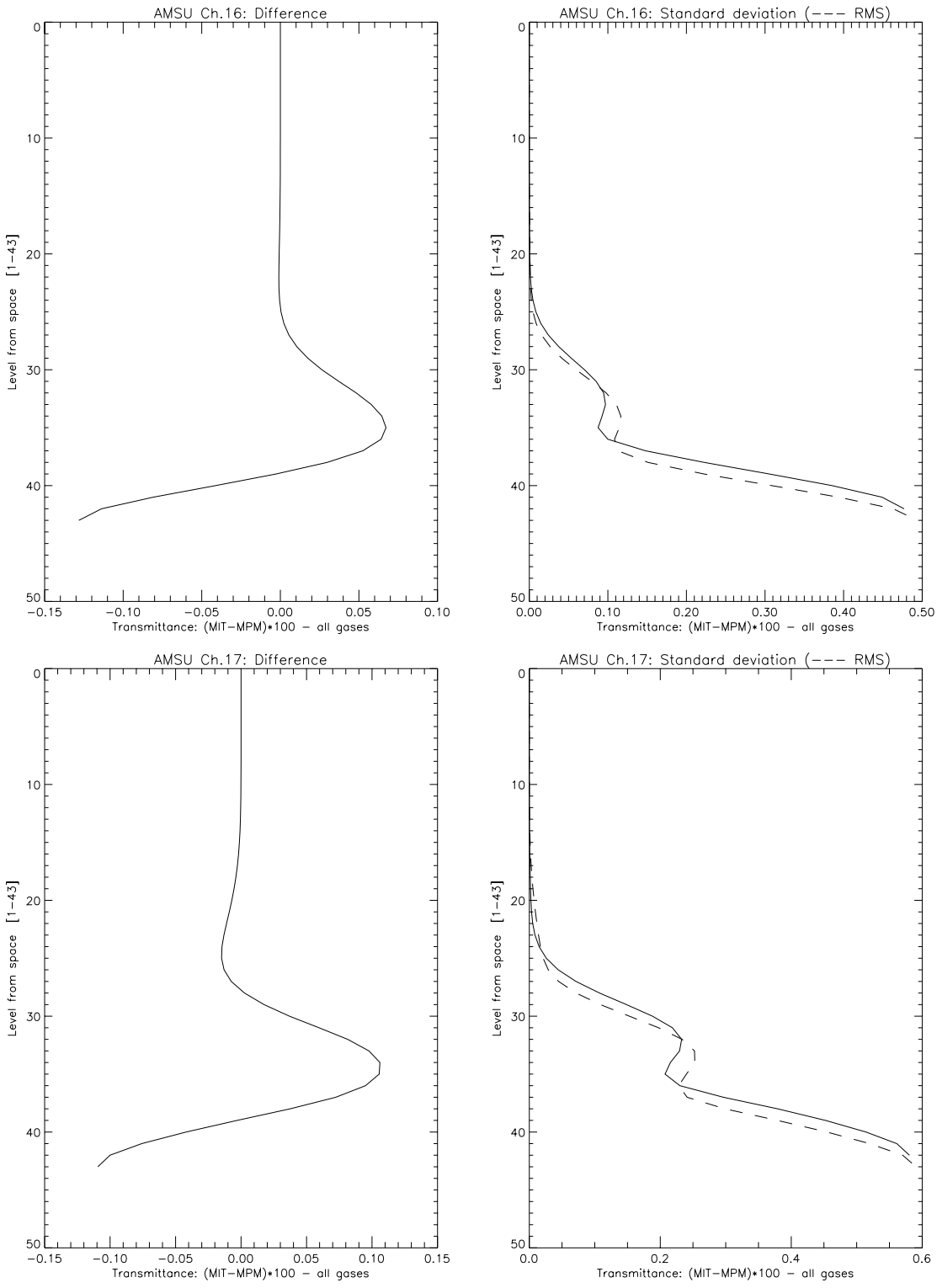

FIGURE 6. *As Figure 5, but for AMSU channels 16-17.*

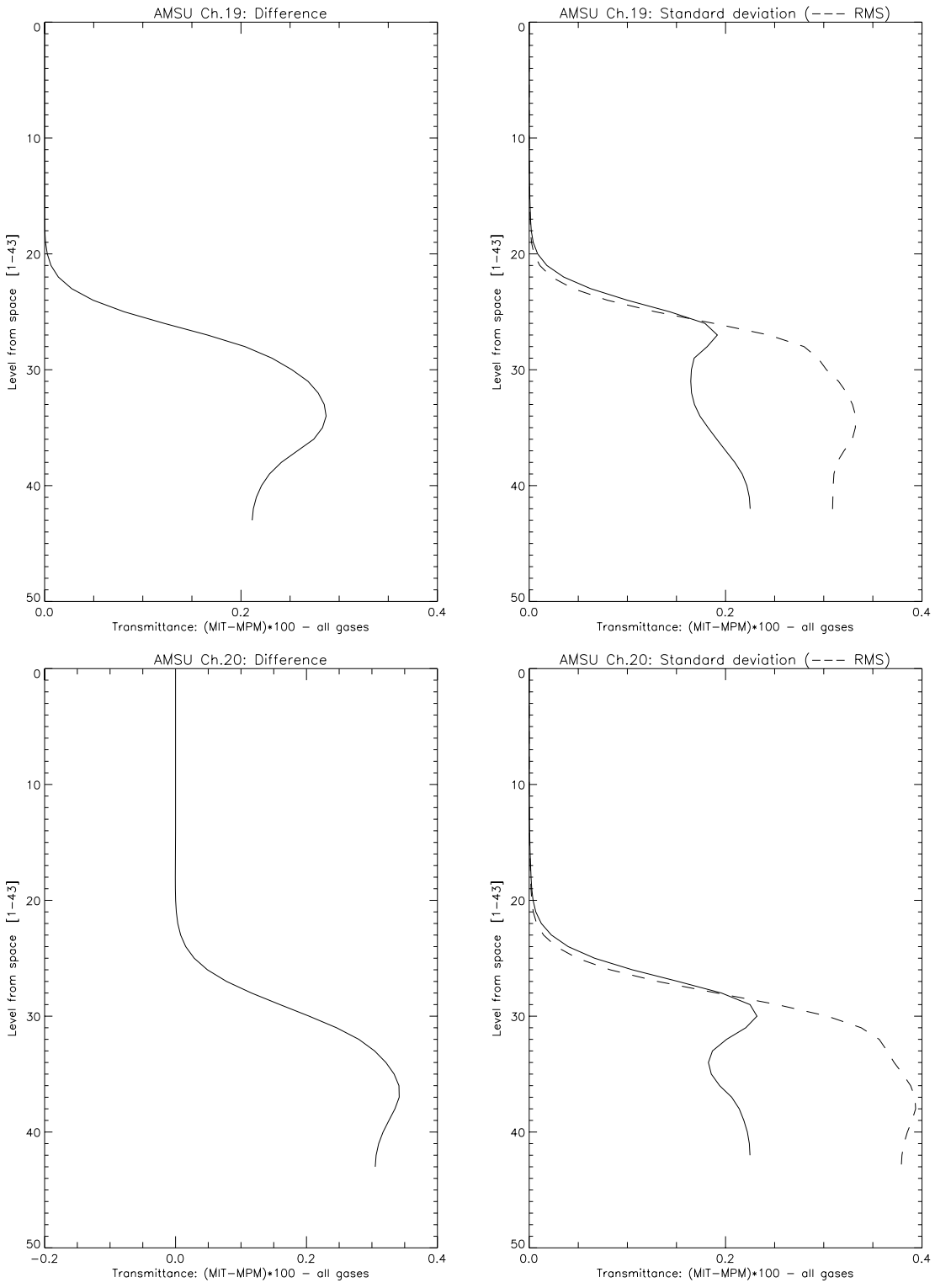

FIGURE 7. *As Figures 5 and 6, but for AMSU channels 19-20.*

6. OTHER INSTRUMENTS: SSM/I AND TMI

Calculations of the difference between MPM and old-MPM were performed for SSM/I and TMI, and particular attention was given to the SSM/I channel near 22GHz, since this had, in the past, proved sensitive to changes in the spectral resolution used in MPM. However, in no case was there any significant difference in the top of atmosphere TBs from these channels. This is unlikely to remain the case for SSMI(S), which is to replace SSM/I, since some of the channel weighting functions peak even higher in the stratosphere than AMSU.

7. CONCLUSIONS

(A) When used in the context of RTTOV-6, it is the LbL *transmittance* from each level to space (i.e. τ_j in (1)) that should be averaged over the channel response, not the layer optical depths. This is the difference between MPM and old-MPM in Table 3, and the effect is greatest, about 0.5 K in both bias and standard deviation, in the AMSU stratospheric channels that sample the steep rise to individual line centres in the O_2 band.

(B) Only when the change in (A) has been made (as in MPM) will there be any effect in using a ratio of transmittances for water vapour in the product rule. Even then, the effect on top of atmosphere TB of using the ratio was very small indeed, probably on account of the near-monochromaticity of the microwave channels in which sidebands are narrow enough to sample individual lines.

(C) Neither SSM/I nor TMI were significantly affected by this change.

(D) Differences of the same order as (A) were also observed for AMSU when the MIT absorption code replaced that of MPM, but this time mainly in the spectral windows due to the self-continuum contribution of H_2O. As shown in Table 6, this amounted to about 0.7K standard deviation (bias small) in AMSU channels 15-17. However, without recourse to measured data for comparison , it remains unclear whether or not this represents an improvement.

(E) Conclusions in (A) and (D) are supported by calculations by Dr G. Deblonde (MSC) using the MSCMWLBL model, which is very similar to MPM.

(F) The MPM model used to generate coefficients for RTTOV-6 includes a simple correction for the Zeeman effect that is significant for AMSU channels 11-14.

ACKNOWLEDGEMENTS

I thank Dr P.W. Rosenkranz (MIT) for supplying the MIT code and for his helpful comments. I greatly appreciate correspondence with Dr G. Deblonde (MSC) and the calculations she made using another model. I also thank Met Office colleagues Dr R.W. Saunders, for suggestions on the scope and content of the report, and Dr A.D. Collard, for much help with MS-Word.

APPENDIX 1 . Technical Details

The LbL model `amsutran43.f` presently used to generate the coefficients for RTTOV-6 has been renamed `amsutran43_MPM.f` for this paper , and it performs the channel averaging on the transmittance. It makes calls to other routines as follows:

```
amsutran43_MPM.f
  call liebe89.f   (water vapour: MPM-1989)
  call liebe93.f   (dry-air: effectively MPM-1992)
```

The original version of `amsutran43_MPM.f` performed the channel averaging on the layer optical depths and has been renamed `amsutrans43_old-MPM.f` for this paper. The calls to the two subroutines were the same.

A modified version of `amsutran43_MPM.f` called `amsutran43_MIT.f` was set up with calls as follows:

```
amsutran43_MIT.f
  call mit_callwat.f  (uses MIT subprogram abh2o.f)
  call mit_calldry.f  (uses MIT subprograms o2abs.f and absn2.f)
```

in which the two new '`mit`' routines make the following conversions:

input water vapour abundance from hPa to g/m^3;
input spectral frequency from Hz to GHz;
output absorption coefficient from Np/km to dB/km.

There are four output transmittance files from `amsutran43_MPM.f`, namely

`amsutrMG_MPM.dat`	(mixed gas channel transmittances, each level to space)
`amsutrWV_MPM.dat`	(water vapour channel transmittances, each level to space)
`amsutrWR_MPM.dat`	(water vapour channel transmittance ratios, each level to space)
`amsutrAL_MPM.dat`	(all gas channel transmittances, each level to space)

and corresponding files from `amsutran43_old-MPM.dat` and `amstran43_MIT.dat` were given similar names but with '`MPM`' replaced by '`old-MPM`' or by '`MIT`' as appropriate.

To compare these models, simulations of transmittance and brightness temperature were performed on the 43 diverse profiles in file `tigr43_43lev.dat`, the 'dependent' set of profiles in the regression used to determine the RTTOV-6 coefficients

A new program `comp.f` was written to read the output transmittance files from the various models and compute difference statistics like (MPM − old-MPM) × 100 averaged over the profile set: namely, average difference, rms difference, standard deviation.

This program was also used to convert, for each profile, the output channel transmittance profile from MPM into an upwelling top of atmosphere TB using fixed representative channel emissivities, and then to calculate the TB difference statistics required.

Finally, new programs `rdata.f` and `rdata_4pv.f` were used to extract concise tables of statistics for both transmittance and TB.

APPENDIX 2. Oxygen Lines

Full attention is given to the detail here to allow model users to transfer more easily between different ways of partitioning the same absorption coefficient. In particular, expressions for the line strength in MPM and MIT are compared both with each other and with the widely used HITRAN database.

Both the MPM and MIT models take spectral line parameters for O_2 that are based on MPM-1992 (*Liebe et al*. 1992). For MPM-1992, the parameters for isolated lines used in MPM-1989 (*Liebe et al*. 1989) were used in a retrieval of new O_2 line coupling coefficients from laboratory measurements. Thus coefficients a_1 and a_2, which govern the line strength (at 300 K) and its temperature dependency, and a_3 and a_4, which govern the line halfwidth at (300 K) and its temperature dependency, are the same in MPM-1989 and MPM-1992 --- whereas a_5 and a_6, which govern the line coupling (at 300 K) and its temperature dependency, have been updated in MPM-1992. Note that, in deriving these parameters, the kelvin temperature T has been replaced in all MPM models by the dimensionless quantity θ defined as $300/T$.

The laboratory measurements reported in *Liebe et al*. (1992) were used to retrieve new line coupling coefficients for 34 lines in the O_2 spin-rotation band, which includes many lines between 50 GHz and 70 GHz and also the line near 118 GHz. In fact *Liebe et al. (*1992) lists new line coupling coefficients for four other lines in the band, these having been extrapolated from the rest (Dr P.W. Rosenkranz, private communication). In this way, there are line coupling coefficients for 38 lines included in both MPM-1989 and MPM-1992, but the integrity of the smaller set of 34 used by the MIT model is unaffected --- using a subset of lines might otherwise be expected to invalidate the set of coefficients, since an overall sum-rule would fail. In fact the MIT model has also, in a trivial rearrangement, replaced a_5 by $(a_5 + a_6)$ and $a_6\theta$ by $a_6(\theta - 1)$, so that a_6 takes account of departures from 300 K.

In *Liebe et al*. (1992) there is an indication (Sec.4.1.2 p.635) that the residual errors for the retrieved line coupling coefficients would be reduced if they and all the line widths in MPM-1992 were multiplied by respective factors of 1.15 and 1.05, and *Liebe et al. (*1993) states (Sec. 2.2.1, p.2) that this has been put through in MPM-1993, though subsequently this has been found to produce some unphysical values (negative) for the absorption coefficient in the range 150-350 GHz (depending on conditions) when O_2 is considered alone. It should be

noted that this lies between the spin-rotation and pure rotation bands of O_2, and so the unphysical contribution to the overall spectrum is very small.

Originally, because MPM had the MPM-1993 code installed for O_2, it also used a back-conversion (using the above factors) in order to invoke the desired original line parameters of MPM-1992. However, there were still small differences from those published in *Liebe et al.* 1992, and the direct installation of the latter in MPM has been one outcome of the present work. In the MIT code itself, a few small changes to the published MPM-1992 have been made in respect of the temperature dependence of the line widths, namely to use $(T_{\rm ref}/T)^1$ in place of $(T_{\rm ref}/T)^{0.8}$ for the line near 118 Hz, and to use $(T_{\rm ref}/T)^{0.8}$ in place of $(T_{\rm ref}/T)^{0.2}$ for the lines at higher frequency beyond the spin-rotation band.

Using the line strength in $\mathrm{cm}^{-1}/(\mathrm{molec.\,cm}^{-2})$ as defined for the HITRAN line database (*Rothman et al.*1992), the absorption coefficient $\sigma(\nu)$ in Np/cm for a single line is given by

$$\sigma(\nu) = \{n_{\rm abs}\} \times \left\{ \frac{8\pi^3}{3hc}\frac{\nu_i}{c}(1-e^{-h\nu_i/kT})(R_i\times 10^{-36})\frac{e^{-E_i/kT}}{Q(T)} \right\} \times \left\{ \mathrm{c}\frac{\nu\tanh(h\nu/2kT)}{\nu_i\tanh(h\nu_i/2kT)}\left(\frac{\pi^{-1}\gamma_i}{(\nu-\nu_i)^2+\gamma_i^2}+\frac{\pi^{-1}\gamma_i}{(\nu+\nu_i)^2+\gamma_i^2}\right)\right\} \qquad \text{(A2.1)}$$

in which the spectral frequency ν, the line frequency ν_i, and the pressure-scaled linewidth γ_i are all in Hz, but compensating factors of $1/c$ and c appear explicitly to allow for the conversion to cm^{-1} as used in HITRAN.

The first set of braces contains the local number density $n_{\rm abs}$ of absorbing molecules. The second set of braces defines the HITRAN line strength, but will only equal the listed value if the temperature T is set to 296 K (the HITRSN reference), and if the isotopic abundance for the radiating molecule (terrestrial percentage) is included. In the third set of braces, the tanh-ratio is a correction for the departure of the spectral frequency ν from the line frequency ν_i used in the strength. The spectral density function, shown in round brackets, is the line shape proper here converted from $1/\mathrm{Hz}$ to $1/(\mathrm{cm}^{-1})$ as mentioned earlier, and normalized to unity over the observable range (ν positive).

In the line strength, the partition function $Q(T)$ is well approximated by QT^r, taking $r=1$ for O_2 (diatomic) and $r=3/2$ for H_2O (asymmetric top), and the balance factor (in round brackets) reduces to $h\nu_i/kT$ in the microwave. The unit for the squared dipole transition amplitude R_i of the line is D^2 (D for debye, $1\mathrm{D}=10^{-18}$ esu cm or erg/gauss) and the final

factor gives the expected fractional population of molecules having the energy E_i of the lower state in the line.

As shown, (A2.1) expresses an approximation to the Van Vleck & Huber (VVH) form for the absorption coefficient that is valid when the line wings are excluded. However, since the tanh-ratio will reduce to another factor of (ν/ν_i) in the microwave, it will take on the Van Vleck & Weisskopf (VVW) form characterized by the squared dependency on the spectral frequency . In the microwave, therefore, we can replace (A2.1) by

$$\sigma(\nu) = \{\, n_{\text{abs}} \} \times \left\{ \frac{8\pi^3}{3kT} \frac{\nu_i^{\,2}}{c^2} \frac{(R_i \times 10^{-36})}{Q(T)} e^{-E_i/kT} \right\} \times \left\{ \mathrm{c} \frac{\nu^2}{\nu_i^{\,2}} \left(\frac{\pi^{-1}\gamma_i}{(\nu-\nu_i)^2+\gamma_i^{\,2}} + \frac{\pi^{-1}\gamma_i}{(\nu+\nu_i)^2+\gamma_i^{\,2}} \right) \right\} \qquad \text{(A2.2)}$$

Turning to O_2 in particular, the MPM absorption coefficient in dB/km, converted from Np/cm by a factor of $10^5 \times 10 \log_{10} e$, is given by

$$\sigma(\nu) = \left\{ 10^6 \log_{10} e \times \frac{4\pi}{c} \nu \times 10^3 \right\} \times \left\{ a_1 \times 10^{-6} P_d \theta^3 e^{a_2(1-\theta)} \right\} \times \left\{ \frac{\nu}{\nu_i} \left(\frac{\gamma_i + Y_i(\nu-\nu_i)}{(\nu-\nu_i)^2+\gamma_i^{\,2}} + \frac{\gamma_i + Y_i(-\nu-\nu_i)}{(\nu+\nu_i)^2+\gamma_i^{\,2}} \right) \right\} \qquad \text{(A2.3)}$$

in which the frequencies are again in Hz but there has been a considerable rearrangement compared to (A2.2), including the installation of the coefficient Y_i that will account for line coupling (*Rosenkranz* 1975, 1988) . The first set of braces reduces to $0.1820\,\nu$, with units that render $\sigma(\nu)$ in dB/km when the other factors are taken into account. Its factor of 10^3 has been borrowed from the second set of braces, which provide the line strength S_{MPM} in kHz when the dry-air pressure in kPa is P_d. The third set of braces includes the line shape in Hz^{-1}, and the resonant part of the line shape has not been normalized here, so the necessary factor of $1/\pi$ has been absorbed elsewhere in (A2.3).

If all of the Y_i were set to zero, and the first set of braces multiplied by $\pi(\nu_i/\nu)$ so that the leading factor in the last set of braces becomes $\pi^{-1}(\nu/\nu_i)^2$, then comparison with (A2.2) would be made easier. Whatever the division of factors between strength and shape, (A2.3) comes from *Rosenkranz* (1975), and will reduce to the VVW case when the line coupling is ignored.

From (A2.2) and (A2.3), the HITRAN and MPM line strengths for O_2 are related at temperature T and dry-air pressure P_d by

$$S_{\mathrm{HIT}} = \frac{4\pi^2 kT\nu_i}{c^2 \times \varepsilon P_d} S_{\mathrm{MPM}} \times 10^{-1} \qquad \text{(A2.4)}$$

where the frequency is again in Hz and ε is the volume fraction of O_2 in air (i.e. 0.209), making εP_d the partial pressure of the absorbing molecules. In S_{MPM}, the coefficient a_1 (in kHz/kPa $\times 10^6$) is defined as

$$a_1 = \frac{2\pi\varepsilon \times \nu_i \times (R_i \times 10^{-36})}{3k^2 \times 300^2 \times e^{a_2} \times (Q_{\mathrm{ox}} \times 300^1)} \times 10^7 \qquad \text{(A2.5)}$$

in which the frequency is in Hz and R_i is in D^2 as before. The O_2 partition function $Q(T)$ is taken to be $Q_{\mathrm{ox}}T^1$ or $(Q_{\mathrm{ox}} \times 300)/\theta$, and the appearance of e^{a_2} in the denominator has allowed the exponent in the second set of braces in (A2.3) to reflect *departures* from 300 K. It is clear from (A2.5) that one scaling factor of θ in (A2.3) comes from the partition function, another comes from the microwave reduction of the balance factor in (A2.1), and the third comes from the conversion of the absorber number density n_{abs} to partial pressure εP_d under the gas law.

The MIT absorption coefficient for O_2 is best interpreted with an eye on both (A2.2) and (A2.3). For a start, it is expressed in Np/km, so the factor of $10^6 \log_{10} e$ in (A2.3) is replaced by one of 10^5 (cm to km). For comparison purposes, therefore an extra factor of $10 \log_{10} e$ (Np to dB) must be attached by the calling code. An additional factor of 10^{-9} arising from frequency considerations will be explained shortly, so there is an overall factor of 10^{-4} to be carried. That said, in the first set of braces in (A2.2), the MIT O_2 code substitutes for the number density n_{abs} using the gas law. In fact, MIT expects the O_2 partial pressure εP_d in hPa, so n_{abs} becomes $10^3 \times \varepsilon P_d / kT$ (by contrast, MPM would expect kPa). Taking this with the overall factor of 10^{-4} mentioned above, MIT replaces n_{abs} by the product of $P_d\theta$ and $10^{-1}\varepsilon/(k \times 300)$, this last having the value 0.5034×10^{12}, which appears explicitly in the code as supplied.

The strength S_{MIT} comes from the second set of braces in (A2.2), but excluding the divisor of c attaching to ν_i, and the Boltzmann factor weighting for the lower state population. Because it reflects the use, in (A2.3), of the dimensionless temperature θ and the linear partition function, it is actually written as

$$S_{\mathrm{MIT}} = \frac{8\pi^3 \nu_i^{\,2} \times (R_i \times 10^{-36})}{3c(k \times 300) \times e^{a_2} \times (Q_{\mathrm{ox}} \times 300^1)} \qquad \text{(A2.6)}$$

with units quoted as $\mathrm{cm}^2\ \mathrm{Hz}$, which as $\mathrm{Hz/(molec.\ cm^{-2})}$ corresponds closely to the HITRAN unit of $\mathrm{cm}^{-1}/(\mathrm{molec.\ cm}^{-2})$.

The third set of braces from (A2.2) is retained intact by MIT, except in three matters. Firstly, it lacks the factor of π^{-1} (i.e. of 0.3183), which has been moved elsewhere. Secondly, the factor of c has been cancelled with one from the denominator of the strength, this for compatibility with (A2.6). Thirdly, the frequency is expected in GHz. This last point is the origin for the factor of 10^{-9} taken into account earlier. For consistency in this report, the frequency will be retained in Hz, and a compensating factor of 10^9 attached. In the end, therefore, if all frequencies were in Hz, MIT would express the absorption coefficient in Np/km in the form

$$\sigma(\nu) = \left\{ 10^{-1} \times \frac{\varepsilon}{k \times 300} \right\} \times \left\{ \left(\frac{8\pi^3 \nu_i^2 \times (R_i \times 10^{-36})}{3c(k \times 300) \times e^{a_2} \times (Q_{\mathrm{ox}} \times 300)} \right) \times \left(e^{-a_2(\theta-1)} \times P_d \theta^3 \right) \right\}$$
$$\times \left\{ 10^9 \times \frac{\nu^2}{\nu_i^{\,2}} \left(\frac{\gamma_i + Y_i(\nu - \nu_i)}{(\nu - \nu_i)^2 + \gamma_i^{\,2}} + \frac{\gamma_i + Y_i(-\nu - \nu_i)}{(\nu + \nu_i)^2 + \gamma_i^{\,2}} \right) \right\} \times \pi^{-1} \qquad \text{(A2.7)}$$

and an additional factor of $10 \log_{10} e$ would convert this to dB/km. The first round bracket in the second set of braces can be recognized as the MIT line strength S_{MIT} in $\mathrm{cm}^2\ \mathrm{Hz}$ from (A2.6). In the MIT code as supplied, the first set of brace is just 0.5034×10^{12}, and the third set of braces omits the factor of 10^9 but demands the frequency in GHz.

Finally, with reference to the expression for a_1 in (A2.5), the conversion from MPM to MIT for O_2 is given by the relation

$$0.182 \times \left(\frac{a_1}{10} \times 10^{-6} \right) = 10 \log_{10} e \times \frac{(0.5034 \times 10^{12})}{\pi(\nu_i \times 10^{-9})} S_{\mathrm{MIT}} \qquad \text{(A2.8)}$$

As justified below, both sides express attenuation per unit pressure (specifically (dB/km)/hPa), and both (at 300K) look for a pressure factor in hPa of $(\nu/\nu_i)(\nu F_i(\nu)) \times P_d$, where $F_i(\nu)$ is the spectral density shown in round brackets in (A2.3). These are magnetic dipole lines and are therefore quite weak. The O_2 band is a dominant spectral feature because of the great abundance of the radiators. To make the numbers more manageable, a_1 has been inflated by a factor of 10^6 in MPM-1992, and it is $a_1 \times 10^{-6}$ that has its basic unit kHz/kPa. Inspection of the first set of braces in (A2.3) reveals that, within 0.182 above, there is the kHz to Hz conversion factor of 10^3, and (A2.8) explicitly shows the divisor of 10 for the kPa to hPa conversion.

APPENDIX 3. **Water Lines**

MPM uses all 30 lines for H_2O listed in MPM-1989 and all line parameters as published. MIT was originally based on *Rosenkranz* (1993) where a set of the seven strongest H_2O lines ($> 0.2\times10^{-21}$ cm^2 Hz) are listed (in Table 2A.2, p.85), to which eight further lines have been added subsequently, making 15 lines in all. These are the 15 lines used in *Rosenkranz* (1998), which states (regarding Eq.1) that the strengths were derived from the HITRAN-1992 database (*Rothman et al*. 1992), and (regarding Eq.3) that the line widths are essentially those used in MPM-1987, the H_2O model used in MPM-1989.

The VVW absorption coefficient is used for H_2O, which means that (A2.3) can be used if all line coupling coefficients Y_i are set to zero. In MPM, the H_2O line strength is that of the second set of braces in (A2.3), but with a_1 and a_2 replaced by b_1 and b_2, and with $P\theta^3$ replaced by $e\theta^{3.5}$, where e is the vapour pressure for H_2O in kPa. The H_2O partition function $Q(T)$ can be written as $Q_{\rm wv}T^{3/2}$ (whereas it was $Q_{\rm ox}T^1$ for O_2), and therefore accounts for the half-power difference in the dependency on θ.

In contrast to its treatment for O_2, MIT uses the number density $n_{\rm abs}$ for H_2O in place of partial pressure as in (A2.2). Therefore, the overall factor of 10^{-4} mentioned earlier and the factor of π^{-1} are brought together (as 0.3183×10^{-4}) to replace the contents of the first set of braces in (A2.7). As mentioned earlier, $S_{\rm MIT}$ is slightly modified from (A2.7) in that $(Q_{\rm ox}\times300^1)$ is replaced by $(Q_{\rm wv}\times300^{3/2})$, and a_2 by b_2. The third set of braces in (A2.2) is modified so that the line shape is truncated at $\nu_i \pm 750$ GHz. This allows for easy installation of the CKD continuum (*Clough et al*. 1989), but has also demanded that the empirical continuum nominally installed (see Appendix 4) be rendered compatible with this line truncation. Finally, corresponding to (A2.8), the MPM and MIT line strengths, this time for H_2O, are related by

$$0.182 \times \frac{b_1}{10} = 10 \log_{10} e \times \frac{(0.5034/\varepsilon)\times10^{12}}{10^4\times\pi(\nu_i\times10^{-9})} S_{\rm MIT} \qquad \text{(A3.1)}$$

where, instead of a_1 in kHz/kPa$\times10^6$, there is now b_1 in kHz/kPa given by

$$b_1 = \frac{2\pi\ \nu_i\times(R_i\times10^{-36})}{3k^2\times300^2\times e^{b_2}\times(Q_{\rm wv}\times\ 300^{3/2})}\times10. \qquad \text{(A3.2)}$$

Compared to the O_2 lines, these lines are strong, and MPM-1989 has not inflated value of b_1 in the same way. Therefore no additional factor of 10^6 appears on the right-hand side of (A3.2),

and no factor of 10^{-6} appears on the left-hand side of (A3.1). Apart from that, the comments made on the units conversions in (A2.8) also stands here. Thus the kHz to Hz conversion is made within the 0.182 factor and the explicit divisor of 10 makes the kPa to hPa conversion. As before, therefore, both sides in (A3.1) are in (dB/km)/hPa and look for a pressure factor of $(\nu/\nu_i)(\nu F_i(\nu))\times P_d$ in hPa.

APPENDIX 4. Dry-Air and Water Vapour Continua

In dry-air, there are two significant sources of broadband microwave continuum. The first is from pressure-induced absorption by N_2, which occurs when a dipole moment, otherwise absent, is induced in the molecule by a collision and allows it to interact with the ambient electromagnetic field during the collision itself – this becomes important only because of the great abundance of this molecule in the atmosphere. The second is non-resonant absorption by O_2, a quantum reinterpretation of the Debye absorption that occurs when energy is extracted from the electromagnetic field as molecules, after a collision, align themselves preferentially along the active field vector. It may be thought of as the result of pressure-broadening on the otherwise unobservable 'line' at zero frequency that arises for O_2 when the initial and final spectral states do not differ.

In MPM, the N_2 absorption coefficient is

$$\sigma_{\text{ind}}(\nu) = \left\{0.182\nu\right\} \times \left\{(1.4\times10^{-12}) P_d \theta^{3.5}\right\} \times \left\{\frac{\nu}{1+(1.93\times10^{-5})\nu^{3/2}}\right\} \qquad \text{(A4.1)}$$

whereas in MIT it is

$$\sigma_{\text{ind}}(\nu) = (6.4\times10^{-14}) \times (P_d + e)\theta^{3.55} \times \nu^2 \qquad \text{(A4.2)}$$

to which the conversion factor of $10 \log_{10} e$ (Np/km to dB/km) must be appended before comparison with (A4.1). The MIT expression comes from *Dagg et al.* (1975) , and may differ from MPM by several percentage points.

In MPM the non-resonant O_2 absorption coefficient is

$$\sigma_{\text{nres-O}_2}(\nu) = \left\{0.182\nu\right\} \times \left\{(6.14\times10^{-5}) \times P_d \theta^2\right\} \times \left\{\frac{\nu\gamma}{\nu^2+\gamma^2}\right\} \qquad \text{(A4.3)}$$

which has the general form of (A2.3) for zero ν_i, given that the effects of line coupling subtract out (*Rosenkranz* 1975 Eq.13, and *Rosenkranz* 1988 p.288). Here the non-resonant halfwidth parameter γ is $0.56\times10^{-3}(P_d + e)\theta^{0.8}$. In MIT, the numerical factor in (A4.3) is the same when converted from Np/km to dB/km, with the same dependency on P_d and θ. However, γ now has $(P_d + e)\theta^{0.8}$ replaced by $(P_d\theta^{0.8} + 1.1e\ \theta)$, the same factor used by both models in the O_2 resonant linewidths.

The line absorption coefficients quoted for HITRAN, MPM and MIT are all invalid in the line wing, where the effect of uncompleted collisions (non-impact effects) will become evident. In

the case of H_2O, this omission is a significant one that is addressed by the inclusion of a continuum term in the absorption coefficient.

In MPM, the continuum absorption coefficient (in dB/km) comes from MPM-1989 and takes the form

$$\sigma_{\text{con}}(\nu) = 0.182\nu^2 \times \left\{ (0.113\times10^{-5})\ eP_d\theta^3 + (3.75\times10^{-5})\ e^2\theta^{10.5} \right\} \qquad \text{(A4.4)}$$

which, in its pressure factors (in kPa), is consistent with (A2.3) (though not derived from it) when $(\nu - \nu_i)^2$ is much greater than γ_i^2, as it would be in the line far-wing. If (A4.4) is interpreted with (A2.3) in mind, then one factor in both terms is e and relates to the absorber abundance, while the other is P_d in the first term (foreign broadening) or e in the second term (self broadening) and relates to the collision rate experienced by the absorber . Once the θ-factors arising from the partition function, the balance factor and the gas law are accounted for, the foreign component in the continuum spectral density (or 'line' shape) is almost independent of temperature T (being $300/\theta$), while the self component still has a strong inverse dependency.

In MIT, on the other hand, the continuum absorption coefficient (in Np/km) takes the form

$$\sigma_{\text{con}}(\nu) = \nu^2 \times \left\{ (5.43\times10^{-10})\ eP_d\theta^3 + (1.8\times10^{-8})\ e^2\theta^{7.5} \right\} \qquad \text{(A4.5)}$$

which, bearing in mind the additional factor of 10^2 that arises when each pressure is expressed in kPa rather than (as here) in hPa, may be compared with (A4.4) by attaching an overall factor of $10\ \log_{10} e$ to convert to dB/km. Furthermore, it is then seen to agree with the substitution of Eqs 5 and 10 into Eq. 6 in *Rosenkranz* 1998 --- although the exponent shown there in Eq.5 should be negative. As described therein, the first (foreign) term in (A4.5) is based on that in MPM-1989, but raised by 15% to allow for the line truncation mentioned in Appendix 3, while the second (self) term is an approximation to the MPM-1993 expression (the 'pseudo-line' of *Liebe et al*. 1993) that is valid for frequencies below 800 GHz.

REFERENCES

Clough, S.A., F.X. Kneizys and R.W. Davies, Line shape and the water vapor continuum, *Atmos.Res. 23*, 229-241, 1989.

Dagg, I.R., G.E. Reesor and J.L. Urbaniak, Collision-induced absorption in N_2, CO_2, and H_2 at 2.3 cm^{-1}, *Can.J.Phys,* 53,1764-1776, 1975.

Eyre, J.R., A fast radiative transfer model for satellite sounding systems, *ECMWF Research Dept. Tech. Memo. 176,* (available from the librarian at the European Centre for Medium-Range Weather Forecasts), 1991.

Liebe, H.J., MPM – an atmospheric miilimeter-wave propagation model, *Int.J.Infrared Milli., 10*,631-650, 1989.

Liebe, H.J., P.W. Rosenkranz and G.A. Hufford, Atmospheric 60-GHz oxygen spectrum: new laboratory measurements and line parameters, *J.Quant.Spectrosc.Radiat.Transfer, 48*, 629-643, 1992.

Liebe, H.J., G.A. Hufford and M.G. Cotton, Propagation modeling of moist air and suspended water/ice particles at frequencies below 1000 GHz, *AGARD 52nd Specialists' Meeting of the Electromagnetic Wave Propagation Panel*, Palma de Mallorca, Spain 17-21 May 1993.

Rosenkranz, P.W., Shape of the 5 mm oxygen band in the atmosphere, *IEEE Trans.Antennas Propag.* AP23, 498-506, 1975.

Rosenkranz, P.W., Interference coefficients for overlapping oxygen lines in air, *J.Quant. Spectrosc.Radiat.Transfer* 39, 287-297, 1988.

Rosenkranz, P.W., Absorption of microwaves by atmospheric gases, Chapter 2 (and appendix) pp.37-90 in *Atmospheric remote sensing by microwave radiometry*, ed. M.A. Janssen, Wiley New York, 1993.

Rosenkranz, P.W., Water vapor microwave continuum absorption: a comparison of measurements and models, *Radio Science 33*, 919-928, 1998.

Rothman, L.S., R.R. Gamache, R.H. Tipping, C.P. Rinsland, M.A.H. Smith, D. Chris Benner, V. Malathy Devi, J.-M. Flaud, C. Camy-Peyret, A. Perrin, A. Goldman, S.T. Massie, L.R. Brown and R.A. Toth, The HITRAN molecular database: editions of 1991 and 1992, *J.Quant. Spectrosc.Radiat.Transfer, 48*, 469-507, 1992.

Saunders, R.W., M. Matricardi and P. Brunel, A fast radiative transfer model for assimilation of satellite radiance observations - RTTOV-5, *ECMWF Research Dept. Tech. Memo. 282,* (available from the librarian at the European Centre for Medium-Range Weather Forecasts), 1999a.

Saunders, R.W., M. Matricardi and P. Brunel, An improved fast radiative transfer model for assimilation of satellite radiance observations, *Quart.J.Roy.Meteor.Soc., 125*, 1407-1425, 1999b.

Susskind, J., J. Rosenfield and D. Reuter, An accurate radiative transfer model for the direct physical inversion of HIRS2 and MSU temperature sounding data, *J.Geophys.Res, 88*, 8550-8568, 1983.